Optical Nonlinearities in InAs/GaAs Injection-Locked Quantum Dot Light-based Emitters

Frédéric Grillot[1,2], Heming Huang[1], Kevin Schires[1], Tagir Sadeev[3], Dejan Arsenijevic[3], and Dieter Bimberg[3,4]

[1]*CNRS LTCI, Télécom Paristech, Université Paris-Saclay, 46 rue Barrault, 75634 Paris Cedex 13, France*
[2]*Center for High Technology Materials, University of New-Mexico, Albuquerque, New Mexico 1313, USA*
[3]*Institut für Festkörperphysik, Technische Universität Berlin, Berlin 10623, Germany*
[4]*King Abdulaziz University, 22254 Jeddah, Saudi Arabia*

grillot@telecom-paristech.fr

ABSTRACT

Frequency conversion using highly non-degenerate four-wave mixing is reported in InAs/GaAs quantum-dot Fabry-Perot lasers. In order to compress the spontaneous emission noise, the laser is optically injection-locked. Under proper injection conditions, the beating between the injected light frequency and the cavity resonant frequency dominates the dynamic behavior and enhances a carrier modulation resonance at frequencies higher than the relaxation oscillation frequency. Conversion efficiencies as high as -12 dB associated to a large optical signal-to-noise ratio of 36 dB are reported. The conversion bandwidth is extended up to 2.1 THz for down-conversion (resp. 3.2 THz for up-conversion) with a quasi-symmetrical response between up- and down-converted signals.

I. INTRODUCTION

Four-wave mixing (FWM), owing to its transparency to modulation formats and the polarization of the input signal, presents an important candidate for WDM systems requiring wavelength conversion, negative frequency chirping and fiber dispersion compensation [1,2]. FWM is also of primary importance for optical nonlinear distortion compensation [3], fast all-optical switching [4], and signal processing in future photonic integrated circuits (PIC) [5]. In semiconductor gain media, FWM is mostly driven by the third-order nonlinear susceptibility $\chi^{(3)}$ contributed by carrier density pulsation (CDP), spectral hole burning (SHB) and carrier heating (CH) [6,7]. Semiconductor nanomaterials like quantum dots (QD) have been demonstrated to be efficient nonlinear optical media, hence exhibiting larger optical nonlinearities with response speeds driven by the dephasing rate through the ultra-fast carrier dynamic [8]. In addition, due to the reduced linewidth enhancement factor, nanostructure materials are useful for eliminating destructive interferences among the different nonlinear processes, hence lowering the asymmetry between up- and down-converted signals [6]. Up to now, most of the experiments have been performed using semiconductor optical amplifiers, taking advantage of their large linear gain and long interaction lengths [9,10]. In contrast, semiconductor lasers are resonant oscillators with more compact dimensions providing lower electrical energy consumption and most importantly much lower amplified spontaneous emission noise, hence substantially improving the OSNR. Although prior arts have mostly concentrated on the use of distributed feedback (DFB) configurations [11,12], it was proved that the corresponding intrinsic nonlinear efficiency remains very sensitive to some complex DFB features such as facet phase effects, and the grating coupling coefficient, which are somewhat difficult to control from device to device without a careful design optimization [13]. In order to increase the optical conversion, injection of an external laser into a Fabry-Perot (FP) laser cavity comprising a nanostructure gain media allows selection of the pump wavelength within the gain spectrum, in order to manipulate the conversion efficiency and control the bandwidth of the converted signals [14,15]. In addition, optical injection-locking allows compressing the spontaneous emission noise and enhancing the dynamic properties of the gain medium. In this work, we present an experimental study of non-degenerate FWM arising in InAs/GaAs QD based light based-emitters. Under adequate injection conditions, it is found that the beating between the injected light frequency and the cavity resonant

frequency dominates the dynamic behavior and enhances a carrier modulation resonance at frequencies higher than the relaxation oscillation frequency. In this work, conversion efficiencies as high as -12 dB with a large optical signal-to-noise ratio (OSNR) of 36 dB are unveiled. In addition, quasi-symmetrical responses of up- and down-conversion efficiencies with bandwidths up to 2.1 THz for down-conversion (resp. 3.2 THz for up-conversion) are reported.

II. DEVICE DESCRIPTION

The active region is a dots-in-a-well structure incorporating 10 InAs QD layers grown by molecular beam epitaxy (MBE) and embedded in InGaAs QWs [16]. The nanostructures' size is typically between 15 to 20 nm wide and 3 to 5 nm high. The dot density is estimated to be $3\text{-}5\times10^{10}$ cm^{-2}. The inhomogeneous broadening retrieved from the photoluminescence response and corresponding to the ground state transition is 50 meV. The optical waveguide is 1.5 mm long, while the ridge waveguide (RWG) structure has a width of 2 µm. The facets are left as-cleaved. All measurements are done at 293 K. Fig. 1 presents the light-current-voltage (LIV) characteristics. The blue line corresponds to the single facet free-space output power while the green one gives the voltage across the junction. A threshold current I_{th} about 30 mA and a differential quantum efficiency of 18% are found. The turn-on voltage is 0.95 V while the series resistance R_s is 6.3 Ω.

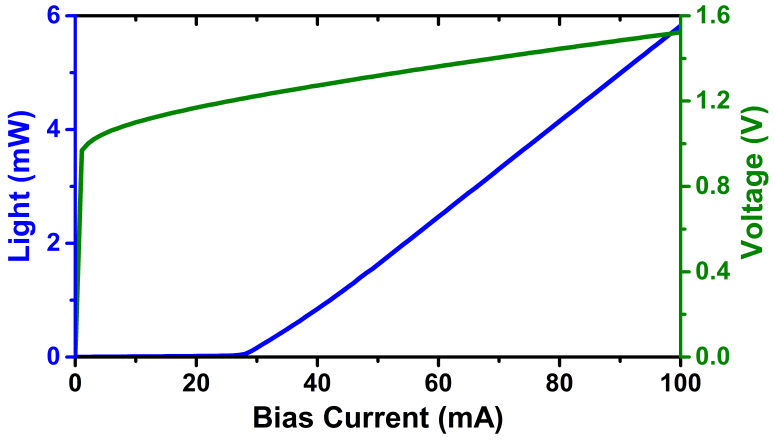

Fig. 1. The LIV characteristics measured at 293 K

The net gain can be retrieved using the Hakki-Paoli method, which is based on the peak-to-valley ratio of the amplified spontaneous spectrum (ASE). Fig. 2 depicts the net modal gain spectra extracted from high-resolution ASE spectra, with varying bias currents from $0.65 \times I_{th}$ to right below I_{th} with a 2 mA current step. The net modal gain at threshold is found to be about 7.5 cm^{-1} at 1305 nm (gain peak).

The below-threshold linewidth enhancement factor (LEF or α_H-factor) is then calculated by tracking the modal wavelength shift and gain change with respect to the current. As such, below threshold, the optical gain of the laser increases with the pump current *I*, while it is clamped above threshold. By measuring the evolution of both the wavelength λ and the gain for various bias currents, the below threshold LEF of the laser is determined by:

$$\alpha_H = -\frac{2\pi}{L\Delta\lambda}\frac{d\lambda/dI}{dg_{net}/dI} \tag{1}$$

where g_{net} is the net modal gain whose variations are depicted in Fig. 2. Fig. 3 represents the evolution of the LEF as a function of the lasing wavelength. After elimination of the thermal effects measured above threshold, the LEF spectrum is found to range from 1.2 to about 3.5 with a value of 2 at the gain peak (1305 nm).

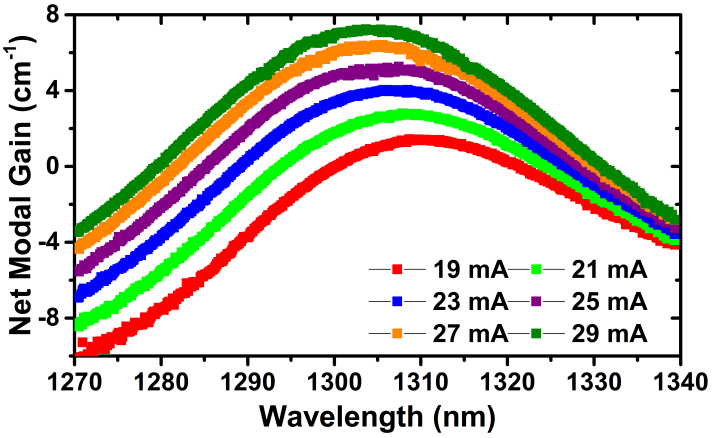

Fig. 2. The measured net modal gain as a function of the lasing wavelength for different bias currents

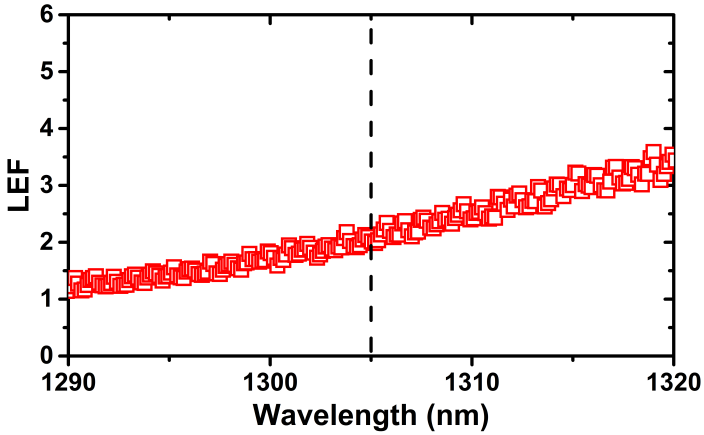

Fig. 3. The measured linewidth enhancement factor (LEF) as a function of the lasing wavelength. The dashed vertical line indicates the position of the gain peak.

III. EXPERIMENTAL RESULTS

The most common way to investigate FWM in semiconductor lasers is based on two external tunable lasers: the pump and probe. In this work, the pump laser is used as a master laser to stably-lock the mode at the gain peak of the slave FP laser, biased well above threshold. Depending on the two degrees of freedom of optical injection, the master laser power and the frequency detuning between master and slave, the slave FP laser can either be unaffected by the injection, oscillate in a periodic or aperiodic fashion, or be injection-locked to the master and emit on a single mode resonant to the injected signal. As an example, Fig. 4 shows the optical spectrum of the InAs/GaAs QD stably-locked laser for which a side mode suppression ratio between the locked and suppressed modes greater than 50 dB is obtained.

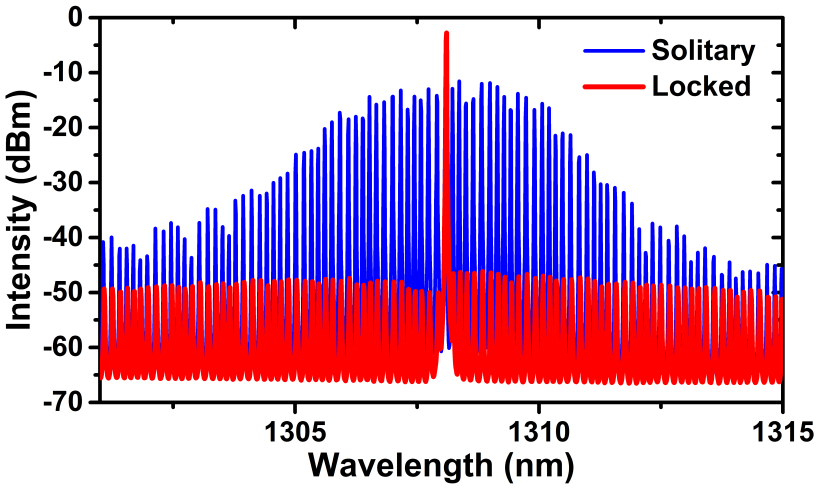

Fig. 4. Output spectra of the solitary InAs/GaAs QD laser (blue) and under optical injection (red)

Fig. 5 shows the optical injection experimental setup used for FWM generation. The light from two tunable lasers is combined using an 80/20 coupler, and is injected into the FP laser cavity through an optical circulator and a lens-ended fiber, the latter being also used to collect the light emitted by the FP. The tunable laser TL1 acts as master laser to lock the longitudinal FP mode at the gain peak and hence generate the pump wave. TL2 is then used as probe for the wave mixing. In what follows, the two QD FP laser are biased at 2.4 × I_{th}. The injected power from TL1 is fixed 1 dB above the free-running power of the FP laser under study. The injected power from TL2 is then chosen 6.3 dB below the free-running FP laser power. The FWM frequency detuning Δf, defined as the frequency difference between TL2 and TL1, is tuned to have the probe coincide with the rejected side-modes of the FP laser, where maximum conversion is obtained. An optical spectrum analyzer (OSA) with a 10 pm resolution is utilized to acquire the optical spectrum of the FP laser, and a power meter (PM) is used to monitor the output power to ensure the stability of the coupling.

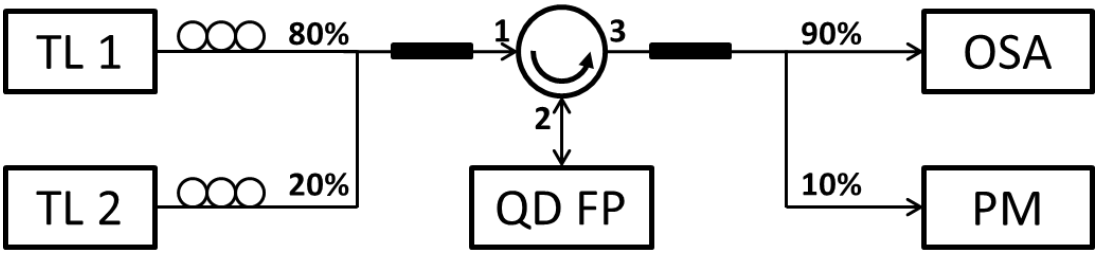

Fig. 5. Experimental setup used for FWM generation with the optical injection configuration

As an example, Fig. 6 represents a typical FWM spectrum corresponding to the up-conversion observed in the QD laser (Δf = -90 GHz). The green peak represents the locked FP mode (pump), and the blue peak is the probe. Stemming from the pump-probe beating, two phase-conjugated signals located at f_{pump} + Δf and f_{probe} - Δf are generated on both sides of the spectrum. The red peak represents the conversion of the probe with respect to the pump.

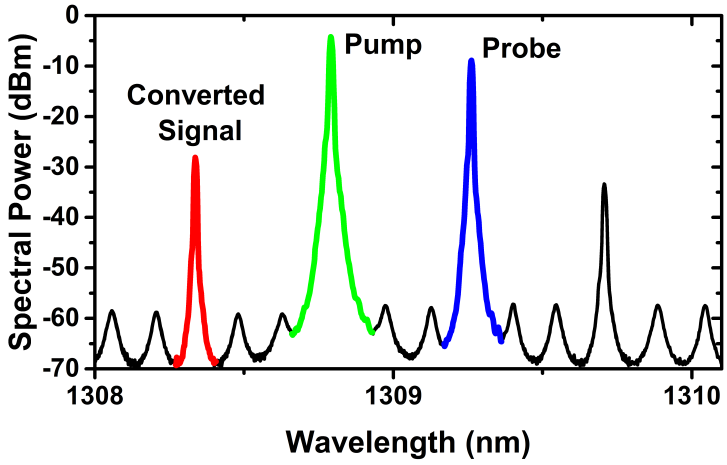

Fig. 6. Measured FWM optical spectra for up-conversion with Δf = -90 GHz under 2.4 × I_{th} and 1 dB pump injection strength.

The conversion efficiency (CE) is usually expressed as:

$$\eta_{CE} = \frac{P_{conv}}{P_{probe}} \tag{2}$$

where P_{conv} and P_{probe} are the optical powers of the converted and probe signals measured from the optical spectra. The OSNR is defined as the peak power ratio between the converted signal and the nearest side modes. Fig. 7 depicts the measured CE and OSNR as a function of the absolute value of the frequency detuning Δf. In Fig. 7(a), two regions can be distinguished: a first decrease of -15 dB/decade (resp. -16 dB/decade) piloted by the CDP, CH, and SHB followed by a faster one of -35 dB/decade (resp. -38 dB/decade) where the hole burning is the dominant process within sub-picosecond timescales. Owing to the low asymmetry in the gain profile and the small LEF, the up- and down-conversion profiles are found to be almost symmetric, meaning that the dominant processes in place, i.e. the CDP and SHB, are almost in phase and interfere constructively. This direction-independent conversion also proves that the lasing wavelength is relatively close to the resonant dot population within the inhomogeneous broadening, as little carrier-induced change in refractive index occurs near the resonance.

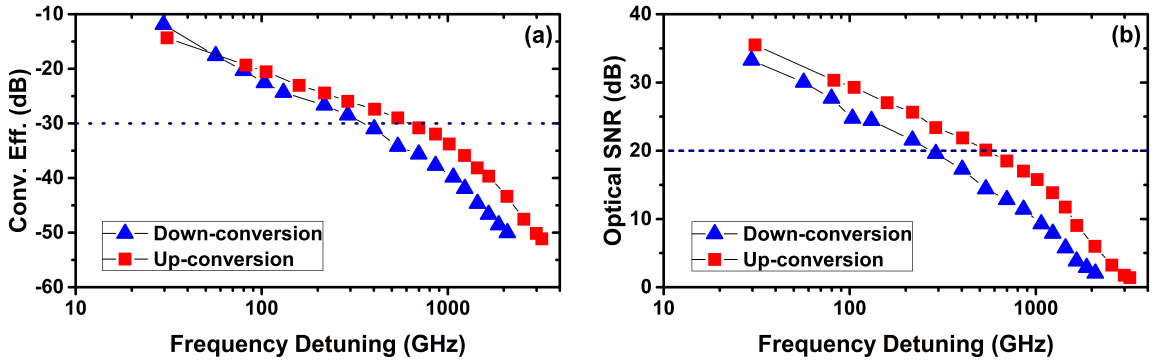

Fig. 7 (a) CE and (b) OSNR as a function of the pump-probe frequency detuning under 2.4×I_{th} and 1 dB pump injection strength. Red square (resp. blue triangle) triangles represent up (resp. down) conversion.

From a quantitative viewpoint, the conversion efficiency reaches a maximum of -12 dB for $\Delta f < 100$ GHz. Overall, the CE is always maintained above -30 dB for down-conversion frequency detunings ranging up to 400 GHz (resp. 700 GHz for up-conversion). For $\Delta f > 1$THz, the SHB dominates, and while the interaction is weaker but still above -50 dB, the conversion largely expands over a much larger bandwidth of up to 2.1 THz for down-conversion (resp. 3.2 THz for up-conversion). Results show that InAs/GaAs QDs used in this work have an appropriate dephasing rate that gives a sufficiently fast response without reducing the amplitude of the conversion. Correspondingly, the extracted OSNR depicted in Fig. 7 (b) proves that the spontaneous emission that is further compressed from the injected field allows maintaining a suppression ratio above the 20 dB level. From (2), it can also be seen that attention has to be paid to the fact that the CE also depends on the pump power and the bias current of the QD FP laser. Fig. 8 shows the evolution of the CE as a function of the frequency detuning under 2.8 × Ith for two different values of the pump injection strength, the pump detuning being fixed at 3 GHz. For both cases, results reveal that the frequency conversion can be affected by the pump injection strength. In particular, for the up frequency conversion, the discrepancy on the CE reaches up to 4 dB when the pump injection strength is increased from 1 dB to 4 dB. Variations of the bias currents also can produce stronger variations on the CE. For instance, Fig. 9 shows the evolution of the CE as a function of the frequency detuning under a pump injection ratio of 1dB, a frequency detuning (-3 GHz) and for two different values of bias current. In this case, the discrepancy can be more important on both sides of the conversion with a maximum difference of 7 dB.

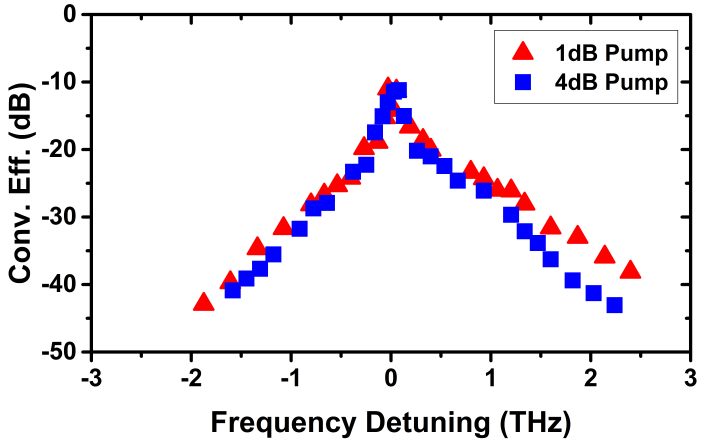

Fig. 8. CE as a function of the pump-probe frequency detuning under 2.8×I_{th} and two different pump injection strengths (the pump detuning is fixed at – 3 GHz).

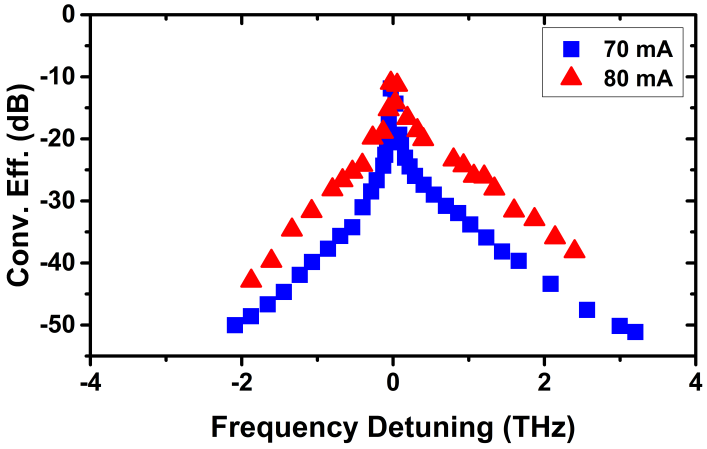

Fig. 9. CE as a function of the pump-probe frequency detuning under the same pump injection ratio (1dB) and a frequency detuning (-3 GHz), and two different bias conditions.

As a conclusion, this result demonstrates the possibility to reach a highly-efficient quasi-symmetrical nonlinear conversion, within the experimental resolution. Such a symmetrical response is fully consistent with the very low LEF measured on this QD laser. Owing to the large number of QD stacks and the high concentration of nanostructures in the active region, reaching the THz-bandwidth does not affect the amplitude of the $\chi^{(3)}$. Finally, comparing the results with SOAs of similar active regions, we found that the optical injection configuration enhances the static conversion and that lower bias currents are required to reach similar bandwidths and conversion efficiencies [9,10].

CONCLUSIONS

This work reports on highly-efficient and symmetric wavelength conversion in optically-injected InAs/GaAs QD FP lasers. Results unveil a maximum conversion efficiency of -12 dB, bandwidths as large as 2.1 THz for down-conversion (resp. 3.2 THz for up-conversion) as well as quasi-symmetrical responses for up- and down-conversions. The results combine at the same time large amplitude, bandwidth and a very good symmetry of the conversion, stemming from the combination of multiple effects. Firstly, the optical injection-locking contributes to enhance the resonance cavity effect and to compress the ASE. Secondly, the discrete energy levels of the QDs concentrate the oscillator strength essentially at the resonant wavelength, leading to a reduced LEF hence improving the symmetry of the conversion. Then, the large number of QD stacks associated to the relatively high density enhances the nonlinear susceptibility. Finally, as opposed to SOAs, optically injection-locked QD lasers require less power to reach similar conversion performance. Since these QD-based emitters operate at 1310 nm i.e. at a wavelength region longer than the bandgap of silicon, this work can be useful for optical signal processing and wavelength converters in silicon photonics integrated circuits.

ACKNOWLEDGMENTS

This work is supported by the Institut Mines Télécom (IMT) through the Futurs & Ruptures program, by the European Office of Aerospace Research and Development under Grant FA9550-15-1-0104 and by the DFG in the framework of the SFB787. The authors also acknowledge E. Decerle from Yenista Optics for providing the external tunable laser and helping us to complete this work.

REFERENCES

[1] C. H. Lee, Microwaves Photonics, CRC Press; 2 edition, (2013).
[2] C.-W. Chow and Y. Liu, Nonlinear Photonic Signal Processing Subsystems and Applications, Advances in Lasers and Electro Optics, pp. 838, INTECH, (2010).
[3] H.-Nguyen Tan, T. Inoue, and S. Namiki, "Highly Cascadable All-Optical Wavelength Conversions of DP-QPSK, DP-16QAM, and DP-64QAM Signals," *European Conference on Optical Communications*, (2015).
[4] K. Weich, E. Patzak ,and J. Hörer, "Fast all-optical switching using tow-section injection-locked semiconductor lasers," *Electron. Lett.*, vol. 30, pp. 493, (1994).
[5] L. Vivien, L. Pavesi, "Handbook of Silicon Photonics," CRC press, (2013).
[6] T. Akiyama, H. Kuwatsuka, N. Hatori, Y. Nakata, H. Ebe, and M. Sugawara, "Symmetric highly efficient (~0 dB) wavelength conversion based on four-wave mixing in quantum dot optical amplifiers," *IEEE Photonics Technol. Lett.*, vol. 14, pp. 1139–1141, (2002).
[7] D. Nielsen and S. L. Chuang, "Four-wave mixing and wavelength conversion in quantum dots," *Phys. Rev. B*, vol. 81, no. 3, pp. 1–11, (2010).
[8] P. Borri, S. Schneider, W. Langbein and D. Bimberg, "Ultrafast carrier dynamics in InGaAs quantum dot materials and devices," *J. Opt. : Pure Appl. Opt.*, vol. 8, pp. 33-46, (2006).
[9] G. Contestabile, A. Maruta, and K. Kitayama, "Four Wave Mixing in Quantum Dot Semiconductor Optical Amplifiers," *IEEE J. Quantum Electron.*, vol. 50, no. 5, pp. 379–389, (2014).
[10] C. Meuer, C. Schmidt-langhorst, H. Schmeckebier, G. Fiol, D. Arsenijevic, C. Schubert, D. Bimberg, "40 Gb/s wavelength conversion via four-wave mixing in a quantum-dot semiconductor optical amplifier," *Opt. Express*, vol. 19, no. 4, pp. 3788–3798, (2011).
[11] A. Mecozzi and R. Hui, "Nearly degenerate four-wave mixing in distributed feedback semiconductor lasers operating above threshold," *IEEE J. Quantum Electron.*, vol. 29, pp. 1477–1487, (1993).

[12] H. Su, H. Li, L. Zhang, Z. Zou, A. L. Gray, R. Wang, P. M. Varangis, and L. F. Lester, "Nondegenerate four-wave mixing in quantum dot distributed feedback lasers," *IEEE Photonics Technol. Lett.*, vol. 17, pp. 1686–1688, (2005).
[13] F. Grillot, "On the Effects of an Antireflection Coating Impairment on the Sensitivity to Optical Feedback of AR/HR Semiconductor DFB Lasers," *IEEE J. of Quantum Electron.*, Vol. 45, pp. 720-729, (2009).
[14] H. Huang, K. Schires, P. J. Poole, and F. Grillot, "Non-degenerate four-wave mixing in an optically injection-locked InAs/InP quantum dot Fabry–Perot laser," *Appl. Phys. Lett.*, vol. 106, p. 143501, (2015).
[15] T. Sadeev, H. Huang, D. Arsenijević, K. Schires, F. Grillot, and D. Bimberg, "Highly efficient non-degenerate four-wave mixing under dual-mode injection in InP / InAs quantum-dash and quantum-dot lasers at 1 . 55 μm," *Appl. Phys. Lett.*, vol. 107, p. 191111, (2015).
[16] A. R. Kovsh, N. A. Maleev, A. E. Zhukov, S. S. Mikhrin, A. P. Vasil'ev, E. a. Semenova, Y. M. Shernyakov, M. V. Maximov, D. A. Livshits, V. M. Ustinov, N. N. Ledentsov, D. Bimberg, and Z. I. Alferov, "InAs/InGaAs/GaAs quantum dot lasers of 1.3 μm range with enhanced optical gain," in *Journal of Crystal Growth*, 2003, vol. 251, pp. 729–736, (2003).